ELSEVIER

Applied Catalysis A: General 127 (1995) 219–232

APPLIED CATALYSIS A: GENERAL

Dehydration of sodium hydroxide and lithium hydroxide dispersed over calcium oxide catalysts for the oxidative coupling of methane

G.C. Maiti [1], M. Baerns *

Lehrstuhl für Technische Chemie, Ruhr-Universität Bochum, D-44780 Bochum, Germany

Received 14 February 1995; accepted 10 March 1995

Abstract

Promotion of CaO by Na^+ or Li^+ leads to an active and selective catalyst for the oxidative coupling of methane into higher hydrocarbons. The structural changes of NaOH- and LiOH-impregnated $Ca(OH)_2$ during calcination were studied by applying differential thermal analysis, IR and X-ray diffraction techniques. The results indicate that both NaOH and LiOH interact with $Ca(OH)_2$ during drying and calcination. The alkali hydroxides tend to dehydrate along with $Ca(OH)_2$ into oxides. In situ infrared spectroscopic studies suggest that dehydration of the mixed hydroxides occurs around 450°C. The measured lattice parameter values indicate that the inclusion of Na^+ or Li^+ ions into the CaO matrix remains very limited. It may be assumed that most of the alkali oxide remains in well dispersed state over the CaO matrix when calcining the samples at 600°C. On increasing the alkali content above 10% no further increase in hydrocarbon selectivity is achieved.

Keywords: Differential thermal analysis; Infrared spectroscopy; Methane oxidative coupling; Sodium/lithium–calcium oxide; Structural change

1. Introduction

Na^+ or Li^+ doped alkaline earth oxides, particularly CaO and MgO have been reported as active and selective catalysts for the oxidative coupling of methane, which seems to be a promising route for converting the vast resources of unused natural gas into higher hydrocarbons or methanol and formaldehyde [1–6]. The structural composition of alkali-ion-doped alkaline earth oxides is still not well

* Corresponding author.

[1] On leave from Physical Research Wing, Projects and Development India, Ltd., P.O. Sindri, PIN 828122, Dhanbad, Bihar, India.

SSDI 0926-860X(95)00071-2

defined. In earlier X-ray diffraction (XRD) studies no definite crystalline phase of sodium or lithium in the mixed oxide catalytic systems were reported [2,6,7]. Attention has been paid mainly to ascribing the catalytic activity and selectivity of the differently prepared mixed oxides to various assumed surface configurations [1–8]. Along with other compounds of sodium, NaOH has been used as an ingredient for the incorporation of Na^+ ions into CaO or MgO matrices and about 10 mol.-% of Na_2O has been considered as a suitable concentration for the preparation of an active catalyst [6,7]. The use of Na_2CO_3 as an ingredient also leads to the formation of NaOH on interacting with starting $Ca(OH)_2$ even at 300°C [9]. For the addition of Li^+ ions, LiOH or Li_2CO_3 have been used as ingredients [8].

The metal hydroxyl bond in alkali hydroxides is mostly of ionic character, which prevents easy dehydration while $Ca(OH)_2$ and $Mg(OH)_2$ easily decompose due to mostly covalent-type bonding. On heating to 780°C LiOH looses water to form Li_2O [10]. For NaOH there are controversial opinions; according to [10] it does not dehydrate but rather tends to dissociate at very high temperatures into the elements. Duval, however, observed dehydration of molten NaOH [11]. The dehydration and any associated structural changes of the parent hydroxide are influenced by the presence of a second oxide [12–15].

In the present communication, results of a study are reported which has been carried out to identify any possible dehydration of NaOH or LiOH with which $Ca(OH)_2$ had been impregnated, by applying differential thermal analysis (DTA), IR and XRD techniques. The results of this study are intended to elucidate the structural changes which occur in different alkali-promoted alkaline-earth-oxide systems used as catalysts in the above mentioned oxidative coupling of methane.

2. Experimental

2.1. Preparation of samples

Two samples were prepared by admixing the aqueous solutions of NaOH and LiOH to solid $Ca(OH)_2$ by the incipient wetness impregnation technique. The samples were oven dried under vacuum at 120 ± 5°C for 20 h resulting in an approximate concentration of 10 mol.-% alkali hydroxide in $Ca(OH)_2$. In the following, the NaOH and LiOH containing samples are designated as A and B, respectively; the sample consisting of parent $Ca(OH)_2$ only, is designated as C. All chemicals used were of analytical grade.

2.2. DTA measurements

These measurements were performed with a controlled-atmosphere differential thermal analyzer (Netzsch STA 410). α-Al_2O_3 was used as a reference material. During calcination under argon atmosphere the temperature was increased at a rate

of 5°C/min. A sample of about 100 mg was used. Some experiments were also carried out in a DSC cell analyzer (Du Pont DTA-900) using gold caps as sample holders. A sample of about 10 mg was used in the DSC cell.

2.3. IR spectroscopic measurements

IR spectra were recorded by a Perkin-Elmer FTIR 1710 spectrometer using a 2 mg sample admixed with 200 mg KBr in an agate mortar and then pelletized in the usual way. The samples were dried for 10 h at 110°C prior to preparing the pellets.

2.4. X-ray diffraction measurements

X-ray diffraction patterns of the samples were recorded in a Philips instrument using a Guinier camera applying crystal reflected monochromatic Cu Kα radiation (operating condition 45 kV, 25 mA). Silicon was used as an internal standard to correct the 2Θ values for experimental errors. The crystal phase compositions were determined by comparing the measured d-spacings with standard ASTM values. The lattice parameter values were determined from corrected values using a suitable computer program. Measurements were made at room temperatures after air exposure.

2.5. Activity measurement

Detailed procedures of catalyst testing were described elsewhere [7]. The samples were calcined in air atmosphere at 750°C for 8 h. The following experimental conditions were applied for catalyst testing: $T = 740$°C, $P_{CH_4} = 0.67$ bar, $P_{O_2} = 0.07$ bar, $P_{N_2} = 0.26$ bar; gas flow was adjusted in such a way that the degree of oxygen conversion amounted generally to more than 90%.

3. Results and discussion

The various measurements of which the results are described and discussed in the following are summarized in Table 1.

3.1. XRD results

The XRD-derived crystal-phase composition and the corresponding lattice parameter values of the samples are shown in Table 2. The XRD patterns for the samples dried at 120°C and calcined at 600°C are depicted in Figs. 1a and 1b, respectively. XRD reflexes at $2\Theta = 103.4°$ for $Ca(OH)_2$ and at $2\Theta = 93.2°$ for the CaO matrix are shown for illustration.

Table 1
Applied techniques for characterizing the samples

Name of the samples	DTA/TG (Netzsch STA)	DSC (Du Pont DTA 900)	IR spectroscopy (Perkin-Elmer FTIR-1710)	XRD studies (Philips Cu Kα)
Sample A, $Ca(OH)_2$ + 10 mol.-% NaOH	25–700°C	25–600°C	IR spectra of oven dried samples and IR spectra in situ at 25, 300, 400 and 450°C to follow dehydration of ν_{OH} band for the samples A, B	XRD patterns were recorded of the samples A, B and C after different heat treatment processes up to 700°C
Sample B, $Ca(OH)_2$ + 10 mol.-% LiOH	25–700°C	25–600°C		
Sample C, pure $Ca(OH)_2$	25–700°C	25–600°C	IR spectra of oven dried and calcined samples	
Pure NaOH	–	25–600°C[a]	IR spectra of oven dried samples	
Pure LiOH	–	25–600°C[a]	IR spectra of oven dried samples	XRD patterns for oven dried samples

[a] Heating and cooling curves.

Table 2
Crystal phase composition and lattice parameter values of sample A, B and C

Name of the sample	120°C			450°C	600°C	600°C
	Crystalline phase	Lattice parameter of $Ca(OH)_2$ phase		Crystalline phase	Crystalline phase	Lattice parameter of CaO, a_0 (Å)
		a_0 (Å)	c_0 (Å)			
Sample A	$Ca(OH)_2$ Na(OH) $CaCO_3$ trace	3.592	4.916	CaO $Ca(OH)_2$ minor $CaCO_3$ trace	CaO $Ca(OH)_2$ trace $CaCO_3$ trace	4.815
Sample B	$Ca(OH)_2$ Li(OH) $CaCO_3$ trace	3.599	4.889	CaO $Ca(OH)_2$ minor $CaCO_3$ trace	CaO $Ca(OH)_2$ trace $CaCO_3$ trace	4.811
Sample C	$Ca(OH)_2$ $CaCO_3$ trace $CaCO_3$ trace	3.590	4.911	CaO $Ca(OH)_2$ minor $CaCO_3$ trace	CaO $Ca(OH)_2$ trace $CaCO_3$ trace	4.817

Crystalline phases of $Ca(OH)_2$ and NaOH are present in case of sample A, oven dried at 110°C. The strongest line for the NaOH phase (dhkl = 2.353 Å) is mainly detectable but others are not very distinct as they have comparatively low intensity ($I/I_{max} < 20\%$). After calcining sample A at 450 and 600°C the XRD patterns indicate the formation of CaO as the major phase along with a minor amount of the $Ca(OH)_2$ phase. However, XRD patterns do not indicate a NaOH phase any more. Similarly for sample B calcined above 450°C the XRD pattern indicates the presence

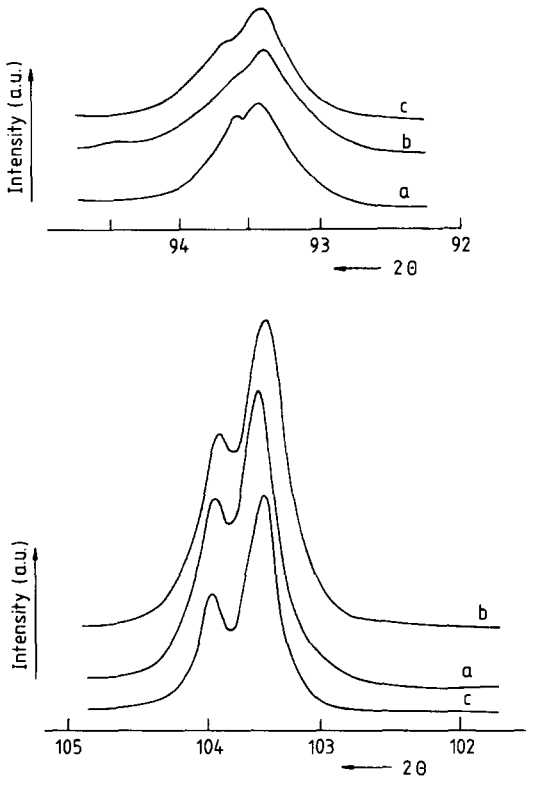

Fig. 1. (a) XRD peak of $Ca(OH)_2$ phase ($2\theta = 93.22$, Cu Kα) in oven dried samples (a: sample C, b: sample A, c: sample B). (b) XRD peak of CaO phase ($2\theta = 103.34$, Cu Kα) after calcining the samples at 600°C (a: sample C, b: sample A, c: sample B).

of the CaO phase; no LiOH phase is detected for the sample calcined at 450°C and 600°C, although the presence of the LiOH phase is observed in the oven dried sample. XRD lines for the LiOH phase are quite weak in case of sample B; when using a sample consisting of 20 mol.-% of LiOH they are more distinct [9]. The disappearance of the alkali hydroxide phases is most probably due to transformation to alkali oxides (see below) being finely dispersed within the CaO lattice so that phase identification is not possible. The peak widths in XRD patterns of the $Ca(OH)_2$ and CaO matrices have been observed to be generally broader in alkali doped samples than that of the pure $Ca(OH)_2$ or CaO matrix (Fig. 1). The line broadening of XRD peaks can be either due to the decrease in crystallite size or due to the development of lattice strain in the presence of foreign ions in the parent matrix. In the case of Li^+ and Na^+ ions impregnated samples A and B there is no decrease in crystallite size of CaO as confirmed from electron microscopic studies. Therefore the extra line broadening may be assigned to an incorporation of Na^+ or Li^+ ions in the $Ca(OH)_2$ and CaO matrices.

The presence of $Ca(OH)_2$ and $CaCO_3$ phases which have been observed after calcination has most probably to be ascribed to formation during handling of the

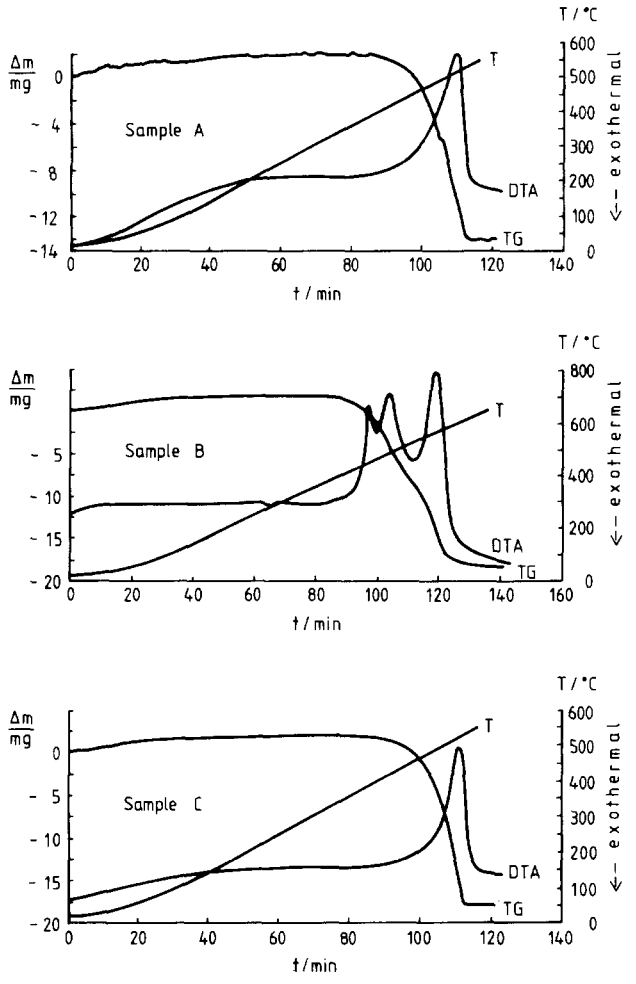

Fig. 2. (a–c) DTA and TG curves obtained under argon atmosphere for samples A, B and C (top: sample A, middle: sample B, bottom: sample C).

sample under ambient conditions since CaO is very sensitive to water vapour and CO_2, specially when calcined at lower temperature.

3.2. *Thermoanalytical results*

Thermoanalytical curves (DTA and TG) for samples A, B and C are shown in Figs. 2a to 2c; as a reference the corresponding data obtained for pure NaOH and LiOH are presented in Fig. 3.

A strong endothermic peak occurs at 520°C for sample A, which can be assigned to the transformation of the hydroxide phase into the oxide state through the dehydration process. The thermogravimetric measurements (Fig. 2a) also indicate a weight loss of 20.5%, which starts above 400°C and reaches its final value above 550°C. The DTA curve does not show any endothermic peak for the melting of the

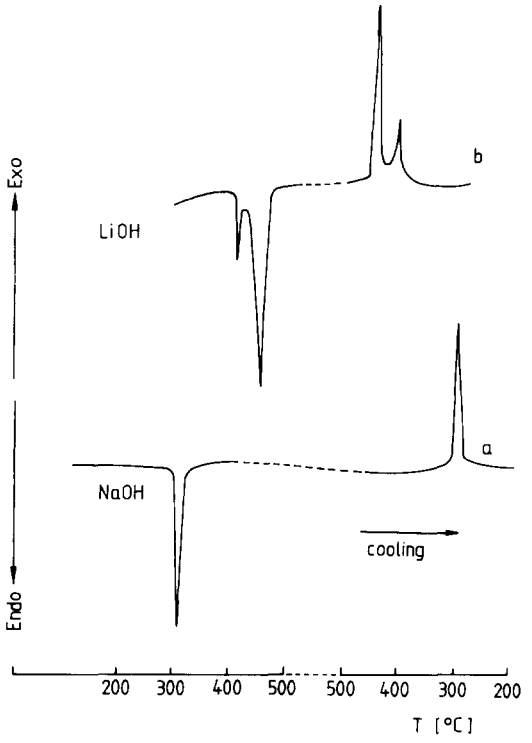

Fig. 3. DSC curves obtained under nitrogen atmosphere for LiOH and NaOH.

NaOH phase, which has been observed as a sharp peak at 310°C for pure NaOH (Figs. 2a and 3); this may be interpreted by assuming that sodium hydroxide interacts with the $Ca(OH)_2$ matrix during wet incipient impregnation and subsequent drying. For sample B a broad endothermic peak with three maxima at 449, 476 and 550°C, respectively, is obtained by DTA (see Fig. 2b). It is difficult to assign each peak separately. However, it may be assumed that the endothermic signal at 550°C is due to the transformation of the hydroxides into their respective oxides. This view is supported by the thermogravimetric data (Fig. 2b) which show a weight loss of 19.8% which starts above 400°C and approaches its final value at about 580°C. The first two endothermic peaks at 449 and 476°C may be assigned to a phase transformation and melting of the LiOH phase. DSC studies for pure LiOH under N_2 atmosphere indicate two strong endothermic peaks at 405 and 440°C and both the peaks reappear as exothermic signals nearly at the same temperatures during cooling (Fig. 3). Again, the first endothermic peak of the DTA curve (Fig. 2b) may be ascribed to some structural change of LiOH while the others may be due to melting of LiOH and the decomposition of $Ca(OH)_2$ to CaO. When considering the thermogravimetric data also dehydration occurs above 400°C and weight loss continues up to 580°C.

The thermoanalytical curve for pure $Ca(OH)_2$ shows a strong endothermic peak at 515°C and the weight loss amounts to 20.1% in the temperature range from 380 to 550°C (Fig. 2c). The endothermic peak maximum for the dehydration of

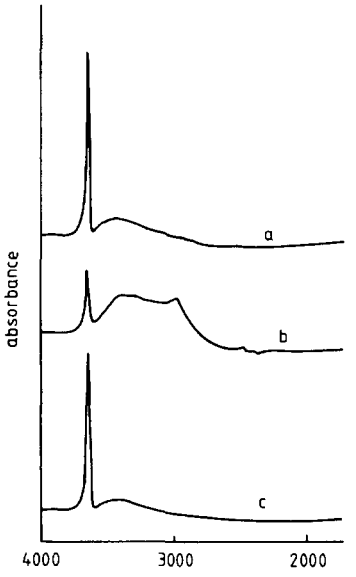

Fig. 4. IR spectra recorded at room temperature of oven dried (120°C) samples (a: $Ca(OH)_2$, b: NaOH and c: $Ca(OH)_2$ + 10 mol.-% NaOH).

$Ca(OH)_2$ depends on the amount of the sample (in DTA studies about 100 mg samples were used); similar observations have been made in thermogravimetry [16,17]. DSC studies indicate a maximum at 435 ± 5°C when ca. 10 mg samples are used. The dissociation pressure of $Ca(OH)_2$ is 1.333 Pa at 390°C [10]. Thus, the dehydration can occur above 400°C. In DTA measurements an onset temperature of 410°C has been noticed. Datta et al. [18] reported that the decomposition of $Ca(OH)_2$ starts above 400°C. Thermogravimetric measurements indicate that the weight loss is nearly the same for both the samples A and B and quite comparable to that of parent $Ca(OH)_2$. However, the weight loss accounted in samples A, B and C (ca. 20%) is lower than expected from theory for the complete dehydration of $Ca(OH)_2$ (24.3%); this can be attributed to the presence of some carbonate impurities in the starting material $Ca(OH)_2$ as identified both in XRD and IR studies.

3.3. IR spectroscopic studies

The IR spectra of catalyst samples A and B, oven dried at 120 ± 5°C are shown in Figs. 4 and 5, and the change in intensity of IR spectral bands during the heat treatment of the samples A and B is illustrated in Figs. 6 and 7, respectively.

Infrared spectra of pure NaOH and $Ca(OH)_2$ as well as of a mixed $Ca(OH)_2$–NaOH (sample A) show strong absorption bands at 3648 cm^{-1} which can be assigned to the stretching vibration of OH groups. Besides this sharp band, a broad absorption band at 3425 cm^{-1} has been noticed for sample A and for pure $Ca(OH)_2$ (sample C). In case of NaOH three maxima at 3391, 3290 and 2980 cm^{-1} have

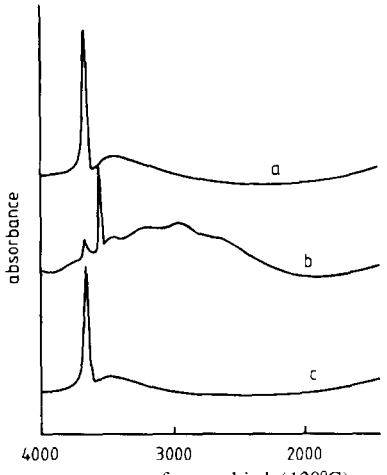

Fig. 5. IR spectra recorded at room temperature of oven dried (120°C) samples (a: $Ca(OH)_2$, b: LiOH, c: $Ca(OH)_2$ + 10 mol.-% LiOH).

been observed in this region of the IR spectrum; these bands can be assigned to associated water molecules through different modes of hydrogen bonding as well as for the hydrogen bonded hydroxyl ions in case of mixed hydroxides systems. A broad absorption band at 1640 cm^{-1} has been noticed for all the samples. Besides these bands, IR spectra show also other bands at 1480, 1420 and 880 cm^{-1} which can be attributed to the presence of carbonate impurities.

The nature of changes in intensity of ν_{OH} bands during heating has been followed at different temperatures for sample A (10 mol.-% of NaOH admixed to $Ca(OH)_2$) (Fig. 6). The results indicate that on heating the sample up to 300°C, there is only a minor decrease in intensity of the ν_{OH} band at 3631 cm^{-1}. The shift in the ν_{OH}

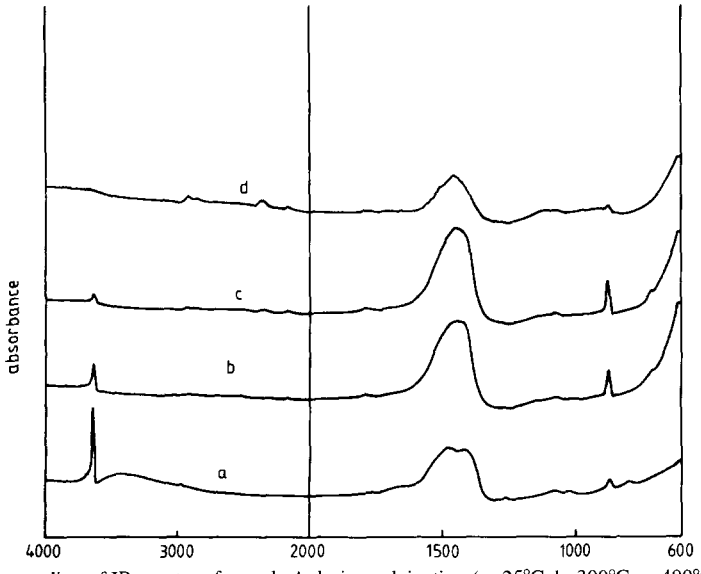

Fig. 6. In situ recording of IR spectra of sample A during calcination (a: 25°C, b: 300°C, c; 400°C, d: 450°C).

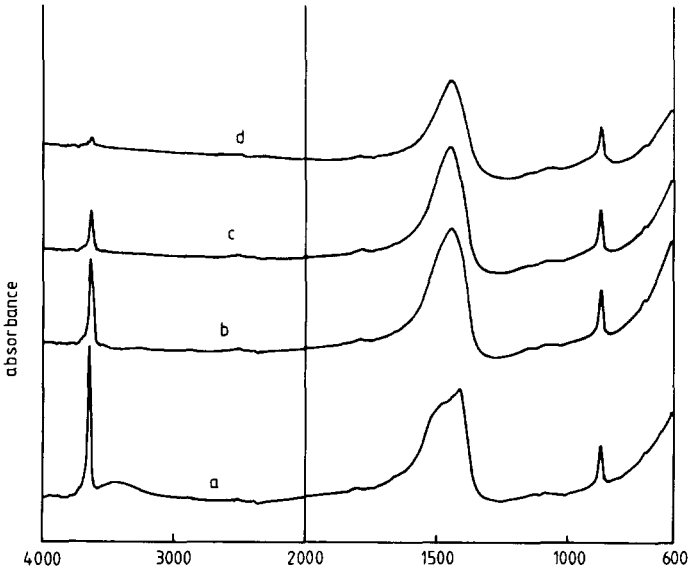

Fig. 7. In situ recording of IR spectra of sample B during calcination (a: 25°C, b: 300°C, c: 400°C, d: 450°C).

band from 3648 to 3631 cm^{-1} at higher temperatures is due to a temperature effect. However, the intensity of the broad band ranging from 3600 to 2800 cm^{-1} has been reduced at 300°C and it is completely absent at 350°C, indicating that the liberation of associated water molecules is completed at 350°C. The intensity of the ν_{OH} band at 3631 cm^{-1} diminishes rapidly with temperature from 350 to 400°C. It is difficult to assign any band within the stretching region at 450°C. There is only a broad noise level, which persists on heating the sample at 450°C during 90 min. The IR spectrum, recorded after 24 h cooling of the specimen under nitrogen, does not show the presence of any band in the stretching region.

The results show that the dehydration of the NaOH–$Ca(OH)_2$ system (sample A) starts above 350°C and is completed at 450°C. As IR spectra do not show any appreciable absorption band in the stretching region after heating at 450°C, it can be presumed that the dehydration of NaOH occurred along with the $Ca(OH)_2$ matrix.

Similar IR-spectroscopic observations have also been noticed in case of the LiOH–$Ca(OH)_2$ system (sample B) (Fig. 7). The pure LiOH and the LiOH–$Ca(OH)_2$ system show a strong absorption band at 3676, 3566 cm^{-1} and 3640 cm^{-1}, respectively. But for sample B the IR spectrum does not show any sharp band characteristic for free LiOH except a broad band ranging from 3600 to 3300 cm^{-1} (Fig. 5). The results may be interpreted by assuming that incorporated LiOH has interacted with the $Ca(OH)_2$ matrix possibly through hydrogen bonding. On heat treatment the intensity of the ν_{OH} band of sample B diminishes gradually. The IR spectra show a strong ν_{OH} band at 3631 cm^{-1} for the sample heated to 300°C. The nearby broad band between 3600 and 3300 cm^{-1} disappears mostly at 350°C and completely at 400°C. The intensity of the ν_{OH} band at 3631 cm^{-1} starts to

diminish at 350°C and reaches the noise level at 450°C. The results indicate that sample B also undergoes complete dehydration on heating at 450°C. The results are in good agreement with those which have been found from DTA and XRD techniques. High temperature IR spectroscopic studies can be considered as a confirmation method because the IR absorption band in the stretching region (ν_{OH}) is detectable even up to a very low level of residual hydroxyl groups at the surface of different oxides.

The experimental results indicate that both, NaOH and LiOH impregnated $Ca(OH)_2$ undergo dehydration together with the $Ca(OH)_2$ phase; it remains, however, an open question to which extent dehydration occurs. In case of pure alkali hydroxides the dehydration does not proceed readily due to their strong ionic bonding. The experimental data, however, suggest that dehydration of NaOH and LiOH can occur in the presence of a $Ca(OH)_2$ matrix. The results can be assigned on assuming that the required protons for the dehydration of the alkali hydroxide phase is supplied from the $Ca(OH)_2$ matrix to LiOH or NaOH sites. The protons in $Ca(OH)_2$ are not rigidly fixed due to their covalent character of the metal–hydroxyl bond. Freund and co-workers [19,20] reported that the dehydration of $Mg(OH)_2$ and $Ca(OH)_2$ occurs through the combination of mobile protons with neighbouring OH sites. The other possibility of alkali hydroxide dehydration is the direct transfer of OH ions from the NaOH matrix to the CaO matrix through the newly created vacant sites in CaO particles where OH ions can be readily converted into O^{2-} ions by the dehydration of hydroxyl ions. The results show that at least part of the sodium hydroxide added to $Ca(OH)_2$ is transformed into Na_2O. Although XRD patterns are not able to indicate the formation of Na_2O or Li_2O phases in the case of samples A and B, however, the formation of Na_2O or Li_2O phase has been identified in samples where higher concentrations of alkali hydroxides prevail [9]. Iwamatsu et al. [5] reported that the addition of alkali ions to MgO causes an extra line broadening in the XRD peak and that the alkali metal ion and Mg^{2+} could be well mixed in the amorphous phase of the hydroxides. At the stage of premature crystallization, alkali metal ions could replace some Mg^{2+} ions in the lattice. We have noticed also an extra line broadening both in oven dried and calcined samples in XRD patterns (Figs. 1a and 1b) In case of lithium-containing $Ca(OH)_2$ (sample B), the broadening is not distinct in the calcined state but the XRD peak is broader in the case of the oven dried sample, which is possibly due to the low ionic radius of the Li^+ ion. The increase in concentration of basic ionic sites of the CaO matrix after calcination can be considered as an indication for the incorporation of Na^+ or Li^+ ions [21].

The measured lattice parameter values are not able to give any clear picture regarding the incorporation of alkali ions into the $Ca(OH)_2$ matrix. No appreciable change in the lattice parameters of $Ca(OH)_2$ has been noticed (Table 2). This is not unexpected as both Ca^{2+} and Na^+ ions have nearly similar ionic radii ($Ca^{2+} = 0.99$ Å; $Na^+ = 0.97$ Å) and Li^+ has a lower ionic radius value with 0.68 Å). Therefore a limited inclusion of Li^+ and Na^+ into $Ca(OH)_2$ should not result

Table 3
Activity and selectivity of alkali compounds on CaO

Name of samples	Activity			Selectivity						
	W/F (g s/ml)	X_{O_2} (%)	X_{CH_4} (%)	C_2H_6 (%)	C_2H_4 (%)	C_3H_8 (%)	C_3H_6 (%)	ΣC_4 (%)	ΣC_nH_m (%)	CO_x (%)
CaO	0.1	94	11	18	33	3.2	–	–	55	45
CaO–NaOH (11.9 %)	0.96	93	15	30	36	5.3	–	4.1	75	25
CaO–LiOH (11.0 %)	1.37	96	16	34	29	5.9	–	6.6	76	24

in any appreciable change in lattice parameter values. The extra line broadening may be assigned to the deformation of the $Ca(OH)_2$ or CaO lattice in the presence of alkali ions. The results show that a solid/solid interaction is developed on admixing the two hydroxides to $Ca(OH)_2$. IR spectroscopic evidence also supports this view as the ν_{OH} bands at 3676 and 3566 cm^{-1} for the LiOH phases are affected on mechanical mixing (Fig. 7). However, in case of NaOH an assignment is difficult as both NaOH and $Ca(OH)_2$ matrices have nearly the same absorption band at ca. 3640 cm^{-1}. Kuroda et al. [22] reported the formation of hydrogen bonding in the case of a MgO surface reaction with adsorbed water molecules. The initial stage of interaction between two hydroxides may be ascribed to the formation of hydrogen bonding and to incorporation of some alkali ions into the CaO matrix during calcination. The chance of formation of a mixed oxide lattice seems to be not existent as both of them are strongly basic. Another possibility would be the diffusion of Na^+ ions into the CaO matrix as they possess similar ionic radii. The ionic diffusion remains also limited as the lattice parameter values of the CaO matrix show only a minor decrease. The measured values are for parent CaO, $a_0 = 4.817$ Å and for the alkali-ions-doped sample A (LiOH), $a_0 = 4.815$ Å and sample B (NaOH), $a_0 = 4.811$ Å. Lunsford et al. [2] suggested from electron spin resonance (ESR) spectroscopic studies that Na^+O^- and Li^+O^- centres are formed in the CaO matrix. However, the results are not very conclusive as Iwamatsu et al. [5] were unable to confirm the formation of such centres from ESR data. It may be therefore assumed that most of the alkali oxides remain in well dispersed state over the CaO matrix, which hinders the identification of any crystalline phase of the alkali oxide component. The high enrichment of the surface with the alkali ions was also reported in earlier works [23,24].

Catalytic activity measurements for the oxidative dimerization of methane indicate that catalysts consisting of alkali and alkaline earth compounds resulted in selectivities up to 76% for the formation of C_{2+} hydrocarbons, which is higher than that of CaO alone as shown in Table 3. It is worthwhile to mention that there is no appreciable influence on catalytic activity and selectivity on raising the alkali concentration above 10% [25,26]. Calcium hydroxide which is transformed into calcium oxide during heat treatment, proved to be a suitable matrix for a limited inclusion of Na or Li ions. It can be presumed that the improvement in the selectivity for the oxidative coupling of methane is due to an increase in surface basicity,

which occurs when alkali ions are incorporated into the CaO matrix. The increase in selectivity with increasing surface basicity was reported in detail in our earlier works [6,7]. Secondly, the doping of alkali ions into the alkaline earth oxide produces a number of low coordination sites, on which the heterolytic activation of methane can occur more effectively [27]. However, the problem still remains how to incorporate an appreciable amount of alkali ions into CaO lattice. Present studies show that the inclusion of Li or Na ions into CaO lattice remains very limited which is possibly due to the strong basic nature and heterovalent character of alkali ions.

The surface composition of the catalyst precursors and the catalysts prior and after the coupling reaction has been reported in our earlier work [25]. Use of high concentration of various sodium compounds does not increase the amount of incorporated alkali ions into CaO matrix. A rather high amount of sodium compounds in the bulk should be avoided because of the build-up of several overlayers of sodium over the CaO matrix as revealed from X-ray photoelectron spectroscopy (XPS) measurements [25]. These excessive amounts of sodium are lost during the calcination and/or catalytic reaction. The loss of alkali ions during the catalytic reaction is a great hinderance for the commercial viability of the alkali ions promoted alkaline earth oxide catalytic systems. The loss of alkali ions above 700°C can be ascribed to their inability to enter into the CaO lattice.

4. Conclusion

Structural studies indicate that the dehydration of NaOH and LiOH can occur in the mixed composites consisting of $Ca(OH)_2$ during the dehydration process. Calcium hydroxide which is transformed into CaO after calcination seems to be a suitable matrix only for a limited inclusion of Na^+ or Li^+ ions. Attempts for increasing the concentration of Li^+ or Na^+ ions in the CaO lattice by using higher amounts of sodium or lithium compounds are not effective since they mostly remain on the surface of newly formed CaO particles. The incorporation of alkali ions into the CaO matrix improves both the catalytic activity and selectivity for the oxidative coupling of methane.

Acknowledgements

This work has been partly supported by the European Union, contract no. EN-3C-0023-D (MB) and 'Fonds der Chemischen Industrie'.

References

[1] G.E. Keller and M.M. Bhasin, J. Catal., 73 (1982) 9.
[2] C. Lin, J. Wang and J.H. Lunsford, J. Catal., 111 (1988) 302.
[3] T. Tagawa and H. Imai, J. Chem. Soc. Faraday Trans., 84 (4) (1988) 923.
[4] T. Doi, Y. Utsumi and I. Matsurra, in M.J. Phillips and M. Ternan (Editors), Proc. 9th Intern. Congr. on Catalysis, Calgary, Vol. 4, 1988, The Chemical Intitute of Canada, Ottawa, 1988, p. 937.
[5] E. Iwamatsu, T. Moriyama, N. Takasaki and K. Aika, J. Catal., 113 (1988) 25.
[6] W. Bytyn and M. Baerns, Appl. Catal., 28 (1986) 199.
[7] J. Carreiro and M. Baerns, React. Kinet. Catal. Lett., 35 (1987) 309.
[8] S.J. Korf, J.A. Roos, N.A. de Bruyn, J.G. van Ommen and J.R.H. Ross, Catal. Today, 2 (1988) 235.
[9] G.C. Maiti and M. Baerns, unpublished results.
[10] P.J. Durrant and B. Durrant, Introduction to Advanced Inorganic Chemistry, Longmans, London, 1962, p. 190.
[11] C. Duval, Anal. Chim. Acta, 16 (1957) 221.
[12] I. Ishii, K. Kamada and R. Furnichi, Thermochim. Acta, 9 (1974) 39.
[13] I. Ishii, K. Kamada and R. Furnichi, J. Chem. Soc. Jpn. (Ind. Chem. Soc.), 74 (1971) 854.
[14] A.K. Galway, in L.E.J. Roberts (Editor), Inorganic Chemistry Series Two: Solid State Chemistry, Vol. 10, Butterworths, London, 1975, pp. 158–180.
[15] J.D. Hancock and J.H. Sharp, J. Am. Ceram. Soc., 55 (1972) 74.
[16] C. Duval, Inorganic Thermogravimetric Analysis, Elsevier, Amsterdam, 1963, p. 270.
[17] F.M. Biffen, Anal. Chem., 28 (1956) 1133.
[18] S. Datta and T. Shirai, Chem. Eng. Sci., 29 (9) (1974) 2000.
[19] F. Freund and H. Wengeler, Ber. Bunsenges. Phys. Chem., 84 (9) (1980) 866.
[20] F. Freund and R. Hoesen, Ber. Bunsenges. Phys. Chem., 81 (1) (1977) 39.
[21] E. Ruckenstein and A.Z. Khan, J. Catal., 145 (1994) 390.
[22] Y. Kuroda, E. Yasugi, H. Aoi, K. Miura and T. Morimoto, J. Chem. Soc. Faraday Trans. 1, 84 (1) (1988) 2421.
[23] E. Ruckenstein and A.Z. Khan, J. Catal., 141 (1993) 628.
[24] T. Grzybek and M. Baerns, J. Catal., 129 (1991) 106.
[25] T. Grzybek, G.C. Maiti, D. Scholz and M. Baerns, Appl. Catal. A, 107 (1993) 115.
[26] J.A.S.P. Carreiro and M. Baerns, J. Catal., 117 (1989) 396.
[27] V.D. Sokolovskii, O.V. Buyevskaya, S.M. Aliev and A.A. Davydov, Stud. Surf. Sci. Catal., 55 (1990) 437.